

Expand-and-Cluster: Exact Parameter Recovery of Neural Networks

Flavio Martinelli*, Berfin Şimşek, Johanni Brea†, Wulfram Gerstner†
 Department of Life Sciences & Department of Computer Sciences
 École Polytechnique Fédérale de Lausanne (EPFL)
 1015, Switzerland

Abstract

Can we recover the hidden parameters of an Artificial Neural Network (ANN) by probing its input-output mapping? We propose a systematic method, called ‘Expand-and-Cluster’ that needs only the number of hidden layers and the activation function of the probed ANN to identify all network parameters. In the expansion phase, we train a series of networks of increasing size using the probed data of the ANN as a teacher. Expansion stops when a minimal loss is consistently reached in networks of a given size. In the clustering phase, weight vectors of the expanded students are clustered, which allows structured pruning of superfluous neurons in a principled way. We find that an overparameterization of a factor four is sufficient to reliably identify the minimal number of neurons and to retrieve the original network parameters in 80% of tasks across a family of 150 toy problems of variable difficulty. Furthermore, shallow and deep teacher networks trained on MNIST data can be identified with less than 5% overhead in the neuron number. Thus, while direct training of a student network with a size identical to that of the teacher is practically impossible because of the highly non-convex loss function, training with mild overparameterization followed by clustering and structured pruning correctly identifies the target network.

1 Introduction

It is known since the 1980s that finding a solution to the XOR problem with gradient descent is easier with a larger hidden layer, even though a minimal network with two hidden neurons is theoretically sufficient to solve the problem [1]. Indeed, even very small networks have a non-convex loss function [2–4]. During the last decades, advances in the theory of artificial neural networks indicate that the loss function is rough for networks of a minimal size, but becomes effectively convex in the limit of infinitely large hidden layers [5–9]. In a teacher-student setup, the complexity of the landscape can roughly be estimated from the ratio between the number of symmetry-induced critical-point manifolds at a positive loss and the number of manifolds at zero loss [10]; at zero loss, teacher and student are functionally equivalent. Importantly, as the degree of overparameterization is increased, the loss landscape undergoes a qualitative change from a ratio larger than one to a ratio smaller than one, suggesting that already for mild overparameterization the landscape is dominated by multi-dimensional zero-loss manifolds [10, 11]. Here we ask whether we can use these theoretical insights to construct a network identification algorithm.

Network parameter identification requires the data to be generated by a neural network; therefore we work in the teacher-student framework. It is arduous to train to zero loss if the student has the same number of hidden neurons as the teacher, however, if the size of the student network is increased by a

*Corresponding author: flavio.martinelli@epfl.ch

†Equal senior author contribution.

factor of two to four, training becomes reliable enough to find a solution close to zero loss. Therefore, we propose to first **expand** the number of neurons in the hidden layer of multiple (N) students until we can train to very low, ideally zero, loss. Using insights on the structure of the zero-loss manifold [10], we then **cluster** similar neurons between different students and prune back to the minimal network size. Thus, the detour via mildly overparameterized networks enables us to reliably find the solution to the original non-convex parameter identification problem (Figure 1).

We present a procedure to extract a functionally-equivalent model of minimal size; this is more than merely matching the teacher’s accuracy on a test set. The desired result is a minimal list of parameters that one can send to a friend, and the friend can consult the teacher to verify that the parameters are correct and the list is minimal. To test the Expand-and-Cluster algorithm, we propose a family of problems with artificial data that enable us to generate hundreds of different regression tasks of variable difficulty, dimensionality, and number of parameters; including generalized XOR-like problems. These tasks are harder than random-teacher models which rarely lead to XOR-like situations. To simplify the procedure, we assume that we know the number of hidden layers and the activation function. For larger-scale applications, we use a regression task to extract parameters of a teacher network optimized on MNIST data. Overall, our examples show that the non-convex network identification problem can be successfully addressed.

Our contributions can be summarized as follows:

- We demonstrate that we can achieve exact, functionally-equivalent *and* minimal size parameter recovery with learning-based methods on toy-sized problems, despite the extreme non-convexity of the problem.
- Mild overparameterization is enough to solve the non-convex problem due to the combinatorial proliferation of global minima predicted by Şimşek et al. [10];
- Our method is orthogonal to other parameter recovery works that are not learning-based, but either rely on special properties of ReLU [12, 13] or perform reconstruction in restricted setups such as committee machines with known layer size [14]. We show successful reconstruction for smooth activation functions on experiments of a similar scale and expand with results on deep fully connected networks.

2 Background and Methods

2.1 Theoretical foundations

Overparameterization consists in increasing the number of parameters of a neural network such that its expressivity is larger than necessary for representing a given dataset [15, 16]. For teacher-student setups, we call a student ‘overparameterized’ if it has more hidden neurons than the teacher in at least one layer. If an overparameterized student network replicates the teacher mapping with zero loss, the space of all possible solutions is fully described by the geometry of the global minima manifold [10]. The global minima manifold contains only two types of hidden units, namely duplicate and zero-type neurons (see theorem 4.2 of Şimşek et al. [10] and Fig. 2A); under the following assumptions: one-hidden layer network $\sum_{i=1}^m a_i \sigma(w_i x)$, infinite input data support, population loss limit, zero bias of all teacher neurons and analytical activation function σ with infinite non-zero even *and* odd derivatives evaluated at zero. The last assumption guarantees that the activation function has no obvious or hidden symmetries around zero. We call activation functions that satisfy these assumptions ‘symmetry-free’.

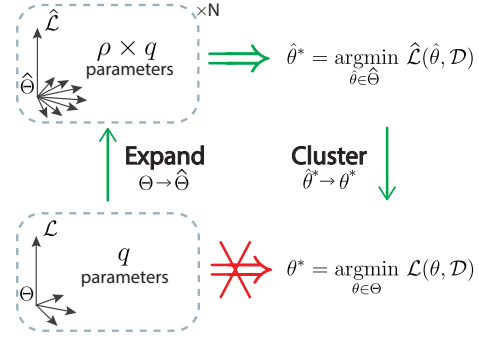


Figure 1: **Expand-and-Cluster**: we overcome the non-convex problem of recovering the q parameters of an unknown network by: (i) expanding the parameter space by a factor ρ to relax the optimization problem, $\Theta \rightarrow \hat{\Theta}$; and (ii) map the solution to the original parameter space through theory-informed clustering, $\hat{\theta}^* \rightarrow \theta^*$. The dataset \mathcal{D} is generated by an unknown network.

The intuition for the result of Şimşek et al. [10] is that, for zero-loss solutions, each teacher hidden neuron $a^* \sigma(w^* x)$ must be replicated in the student by a *duplicate-type* group of one or more units, contributing $\sum_i a_i \sigma(w_i x)$. The duplicates’ input weight vectors are all aligned with the teacher neuron, $w_i = w^*$, while their weighted contribution equals the teacher neuron’s output weight $\sum_i a_i = a^*$. In the same student there can also exist *zero-type* neuron groups with a null contribution to the student input-output mapping, characterized by $w_1 = \dots = w_g$, $\sum_i a_i = 0$. Neuron types from Şimşek et al. [10] but in the presence of biases are summarized in Figure 2A. The assumption of symmetry-free activation function σ is critical because, for example, a student network with tanh units could also contain anti-symmetric input vectors with a switch of output signs.

In this paper, we drop several of the above assumptions to fully reconstruct a teacher network by identifying duplicate neurons while pruning all other superfluous hidden neurons.

2.2 Artificial data in teacher-student networks

To investigate the advantages of overparameterization as a function of layer size, we devised a series of very challenging tasks inspired by the parity-bit problem (or multidimensional XOR), known as a difficult problem for neural networks [1]. To create tasks of variable difficulty, we adapted the problem into a regression format using the following procedure:

All tasks with artificial data have d -dimensional uniformly distributed input data in the range $x_i \in [-\frac{1}{\sqrt{3}}, \frac{1}{\sqrt{3}}]$. A specific task is defined by the parameters of a teacher network. Each hidden neuron i of the teacher is randomly sampled from a set of input weights $w_i \in \{-1, 0, 1\}^{d_{in}}$, output weights $a_i \in \{-1, 1\}$ and biases $b_i \in \{-\frac{2}{3}\sqrt{3}, -\frac{1}{3}\sqrt{3}, 0, \frac{1}{3}\sqrt{3}, \frac{2}{3}\sqrt{3}\}$. We repeat the sampling if two hidden neurons are identical up to output weights signs to avoid two hidden neurons canceling each other. The resulting input weight vectors w are first normalized to unity and then both w and b are multiplied by a factor of 3. The above procedure yields hyperplanes in direction w located at a distance $|b|/||w||$ from the origin, and a steeply rising (or falling) activation on the positive side of the hyperplane. Finally, analogous to batch normalization, the output weights and biases are scaled such that the output has zero-mean and unit variance when averaged over the input distribution: $a \leftarrow a/\text{std}(y)$ and $b_2 = -\langle y \rangle/\text{std}(y)$, where y is the output vector of the network. We study teachers with input dimensionality $d_{in} \in \{2, 4, 8, 16, 32\}$ and hidden layer size $r \in \{2, 4, 8\}$. Figure 4A shows examples of different teachers with input dimension $d_{in} = 2$ and a single hidden layer. We use the symmetry-free activation function $\sigma = \sigma_{sig}(4x) + \sigma_{soft}(x)$, where $\sigma_{sig} = \frac{1}{1+e^{-x}}$ and $\sigma_{soft} = \log(1 + e^x)$ for all our simulations unless specified otherwise. The above construction of hidden neuron parameter vectors can be generalized to multi-layer teachers by stacking the procedure (further details in appendix A.5.2).

Our construction yields XOR-like and checkerboard-like structures where hyperplanes are parallel to each other and divide the input space into separate regions. In contrast to our approach, constructing shallow networks with randomly drawn input weight vectors yields easy tasks since all weights tend to be orthogonal [17–19] and it is known that randomly initialized deep networks tend to behave as constant random functions [20], yielding uninteresting data-generator models. In contrast to committee machines [14], our artificial tasks are more difficult since the output neuron is not merely averaging the contributions of the hidden neurons.

2.3 MNIST regression

To extend the procedure beyond artificial tasks, we also recover parameters of networks trained on the MNIST dataset [21]. We pre-trained teacher networks of either 10, 30, or 60 hidden neurons on MNIST (after removal of the uninformative input pixels, Fig. S5) with standard training procedures. We then used input-output pairs generated by the last layer of the teacher network to define a regression task on which we trained student networks. For our method to work it is crucial that we have access to the classifier’s probabilistic output (e.g. the values after the softmax operation or multiple accumulated decisions of a stochastic classifier) and not only the most probable class (e.g. values after argmax operation) which would make parameter recovery impossible.

2.4 Related Work

1. Pruning: Commonly used pruning methods are heuristic and based on pruning weights [22–24], whereas we propose a theory-based [10] approach that removes entire units (structured pruning) potentially relevant for hardware implementations [25]. Our Expand-and-Cluster method reconstructs a minimal network by positively selecting commonly occurring hidden neurons across a set of overparameterized student networks, as opposed to other structured pruning algorithms [26–28] which remove putatively redundant units; Srinivas and Babu [29] also prune neurons based on weight similarity. In contrast to Ankner et al. [30], who link prunability to data dimensionality, we show a link to data complexity for fixed dimensionalities.

2. Loss landscape and overparameterization: Neural network landscapes exhibit a cusp-like transition from under- to over-parameterization [31, 32], related to double-descent phenomena [33]. Overparameterized solutions found by different random initializations are similar to each other in the function space [34] and have been *approximately* mapped to each other by permutation of hidden neurons [35–40]. In the teacher-student setting, different zero-loss solutions are *exactly identical* to each other up to duplicate-type neurons, zero-neuron addition and permutation symmetry in the population loss limit [10]. However, convergence to a zero-loss solution can be hindered either due to the emergence of local minima [41] or the flatness at the bottom of the landscape [42].

3. Non-convex optimization: Many non-convex optimization problems are tackled with the following strategy: (i) expand, or *lift*, to a higher dimensional space in order to relax the problem and guarantee convergence to global minima; (ii) map, or *project*, the relaxed solution to the original space by exploiting the problem’s intrinsic symmetries and geometry [43]. This approach is used in applied mathematics [44, 45], computer vision [46], nonlinear programming [47–49], control theory [50], machine learning [43, 51] and many others³. Despite the above-mentioned achievements, for neural networks, the picture is far from complete. Unlike infinitely-wide neural networks [5], the loss functions of finite-width neural networks exhibit essential non-convexity so that the gradient flow converges to many fundamentally different solutions depending on the initialization [41, 52, 53]. Shallow networks with polynomial activation functions can be globally optimized under certain guarantees by lifting the optimization problem to tensor decomposition [51, 54]. Even though the mildly overparameterized regime is non-convex, we show that we can exploit its reduced complexity (compared to non-overparameterized problems [10]) to find zero-loss solutions.

4. Interpretability: Explaining in qualitative terms the behavior of single neurons embedded in deep networks is a challenging task [55, 56]. For example, in symbolic regression, small networks with vanishing training loss are desirable for interpretability [57]. We provide precise mathematical explanations of all hidden neurons found in zero-loss overparameterized student networks in relation to a teacher network of minimal size; going beyond the notion of ‘superimposed’ features described in Elhage et al. [58]. We follow the terminology of [10] and use the terms duplicate or zero type neurons which are related to ‘Monosemantic’ [59] and ‘Frivolous’ [60] units found in various settings.

5. Functionally Equivalent Model Extraction: Our paper focuses on functionally equivalent extractions, that is retrieving a model \mathcal{M} such that $\forall x \in X, \mathcal{M}(x) = \mathcal{M}^*(x)$, where $\mathcal{M}^*(x)$ is the target model. This type of extraction is the hardest achievable goal in the field of Model Stealing Attacks [61], using only input-output pairs [13]. In addition, out of all the functionally equivalent models that we describe in Section 3.1, we extract the one of *minimal size*. Conditions for neural network identifiability and their symmetries have been studied theoretically for different activation functions [62–72], although overparameterized solutions were not considered. To the best of our knowledge, existing functionally equivalent extractions of *trained networks* rely on identifying boundaries between linear regions of shallow ReLU networks [13, 73], with partial success for deep ReLU networks [12]. Janzamin et al. [51] show a theoretical reconstruction based on third-order derivatives. Fornasier et al. [14], building upon [74–77], propose an identification method for wide committee machines (shallow networks with unitary second layer weights) and unit norm teacher weights, where knowledge of the teacher layer size is necessary. We are the first to propose an exact recovery method for arbitrary activation functions on shallow and deep fully connected networks of unknown layer widths, with successful reconstructions of networks trained on MNIST. Our method is learning-based and fundamentally different from the known approaches. However, none of these methods were shown to work in large-scale applications.

³A curated list of solvable non-convex optimization problems can be found here: <https://sunju.org/research/nonconvex>

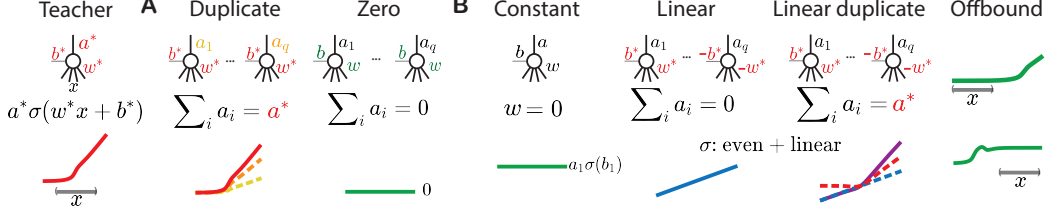


Figure 2: **Catalog of neuron types near zero loss:** with σ analytical, near-zero loss overparameterized students can only contain a handful of neuron types. On the left, a teacher neuron is defined along with a sketch of its output, the grey bar indicates the finite input support x to the neuron; the same color-coded letters indicate equal quantities. **A) Neuron types from Şimşek et al. [10] adapted with biases:** *duplicate-type* neurons combine together to replicate a teacher neuron by copying its weight vector w^* and bias b^* , their activations a_i sum up to the teacher activation a^* . *Zero-types* have aligned weight vectors and biases but cancel each other via output weights. **B) Additional neuron types:** *constant-types* contribute a fixed amount to the next layer by learning a null vector. Only in the presence of even + linear activation functions, such as GELU, *linear-type* groups combine in a way to contribute a linear function, while *linear duplicate types* replicate the teacher neuron summed to an extra linear component. *Offbound-types* appear at non-exact zero loss and are characterized by having the nonlinearity placed away from their input support.

3 Results

3.1 Neuron types near zero-loss

We extend the categorization of neuron types of Şimşek et al. [10] to neurons with *bias*, *finite* input data support and analytical activation functions that contain one *symmetry* due to infinite even or odd non-zero derivatives. This generalization includes commonly used activation functions such as GELU, sigmoid, tanh, softplus. The catalog of new neuron types is sketched in Figure 2B.

In the case of a teacher neuron with bias $a^* \sigma(w^* x + b^*)$, a group of *duplicate-type* $\sum_i a_i \sigma(w_i x + b_i)$ has input weight vectors and biases aligned to the teacher: $w_i = w^*$, $b_i = b^*$, $\sum_i a_i = a^*$, while the new *zero-type* group has aligned, but arbitrary, weights and biases $w_1 = \dots = w_q$, $b_1 = \dots = b_q$, $\sum_i a_i = 0$. With biases, *constant-type* student neurons can also arise: they have vanishing input weights $w = 0$ and contribute a constant amount of $a \sigma(b)$ to the next layer; to keep an exact mapping of the teacher, this constant contribution must be accounted for in the next-layer biases.

GELU or softplus teacher neurons can be written as a combination of a linear and an even function: $a^* \sigma(w^* x + b^*) = a^* c_1 \cdot (w^* x + b^*) + a^* \sigma_{\text{even}}(w^* x + b^*)$, where c_1 is the slope of the linear approximation around 0. The even symmetry allows student neurons to combine in groups of aligned, $w = w^*$, and opposite, $w = -w^*$, input weight vectors and biases (see appendix A.1.1 for details). If in such a group the output weights sum to zero, we obtain a *linear-type* group that contributes a linear function to the next layer. To guarantee an exact mapping of the teacher, there must be another *linear-type* group in the same layer contributing the exact opposite linear term. Alternatively, if the sum of the output weights matches the teacher output weight, then the neuron group is a *linear duplicate-type*, replicating a teacher neuron up to a misaligned linear contribution; the latter can be accounted for by another linear group in the same layer. A numerical example of different neurons found by a softplus student is shown in Figure S6.

Tanh and Sigmoid can be treated similarly: student neurons can group with aligned and opposite weight vectors and combine to form constant types or duplicate plus constant. They are described in detail in the appendix along with a categorization of all commonly used activation functions (appendix A.1.2).

Finally, in near zero-loss solutions, students may have *offbound-type* neurons characterized by being almost constant, linearly increasing or decreasing (depending on the asymptotic behavior of the activation function) in regions of the input space with actual data, which is reminiscent of the dead ReLU phenomenon. The output of groups of *offbound-type* neurons can synergize so as to contribute constant amounts, which can be compensated by bias adjustments in the next layer; see Figure 2.

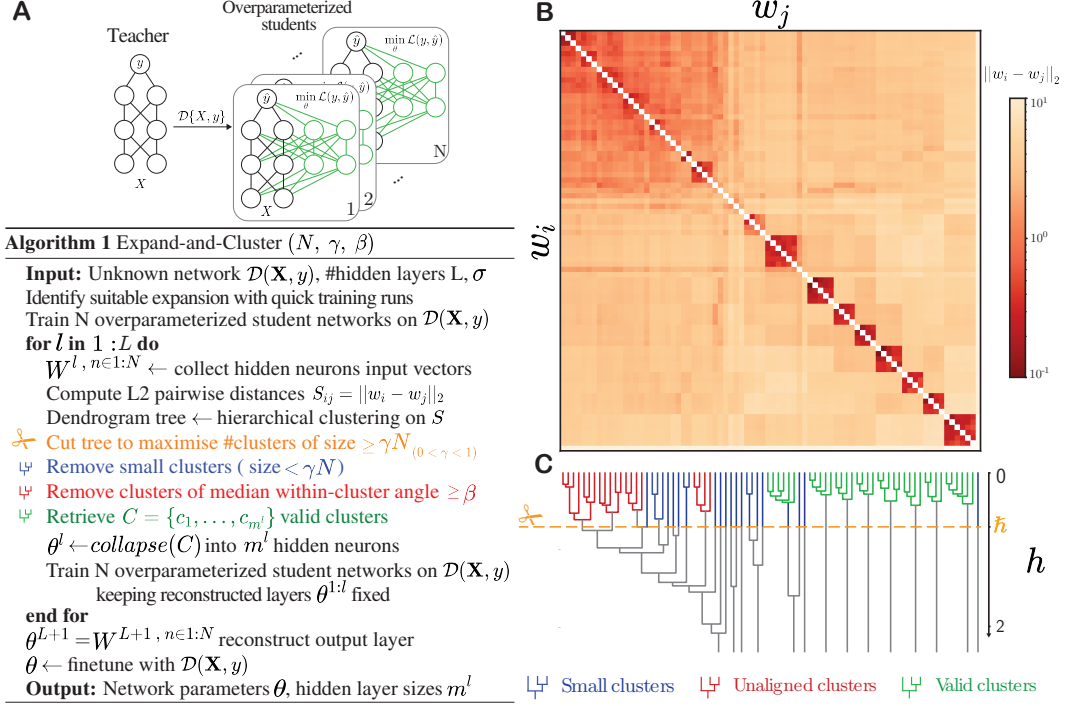


Figure 3: **Parameter identification with Expand-and-Cluster.** **A) Training scheme:** once an overparameterization factor yields near-zero training losses, train N overparameterized students on the teacher-generated dataset $\mathcal{D}(\mathbf{X}, y)$; **B) Similarity matrix:** ℓ_2 -distance between hidden neurons' input weight vectors of layer l for all N students. Large-sized clusters (red and green) are good candidate weight vectors. **C) Dendrogram obtained with hierarchical clustering:** the selected linkage threshold is shown in orange. Clusters are eliminated if too small (blue) or unaligned (red), the remaining clusters are shown in green.

3.2 Expand-and-Cluster algorithm

We recall that the only way an overparameterized student can reach zero loss is by representing all the neurons at least once; see Section 3.1. If a student can be trained to exact zero loss, which is possible in small toy setups, it is almost trivial to identify the different neuron types, including the teacher neurons (see a numerical example in Fig. S6). However, in practice and even in larger tasks with artificial data, overparameterized networks are difficult to train to exact zero loss because of computational and memory budgets. Therefore we need ways to identify the teacher neurons from imperfectly trained students. These students present approximate duplicates of teacher neurons and neurons of other types that point in arbitrary directions. In a group of N imperfectly trained students, neurons that approximate teacher duplicates form clusters while other neurons do not, since they are not aligned between students. Therefore we propose the following clustering procedure (Fig. 3):

Step 1: Expansion phase. Rapidly train a sequence of networks with increasing sizes of hidden layers to a fixed convergence criterion. To do so, use teacher-generated input-output pairs, $\mathcal{D} = \{\mathbf{X}, y\}$, and minimize the mean square error loss with standard gradient descent methods. This expansion phase allows finding a network width m at which convergence to nearly zero loss is possible (Fig. S3B).

Step 2: Training phase. Train N students of L layers, width m , on $\mathcal{D} = \{\mathbf{X}, y\}$ to minimize the mean square error to the lowest value achievable by the chosen optimizer (Fig. 3A).

Step 3: Clustering phase. Collect the first hidden layer neurons of the N students, then cluster the input weight vectors with hierarchical clustering on the L2 distance. With a threshold selection criteria that maximizes the number of large clusters (size $\geq \gamma N$, $0 < \gamma \leq 1$), obtain groups of aligned weight vectors; these clusters should include all duplicate teacher neurons. Proceed to filter out clusters whose elements are not aligned in angle (median alignment $\geq \beta$), removing eventual zero or constant type neuron clusters. Then, merge each remaining cluster of duplicate neurons into single

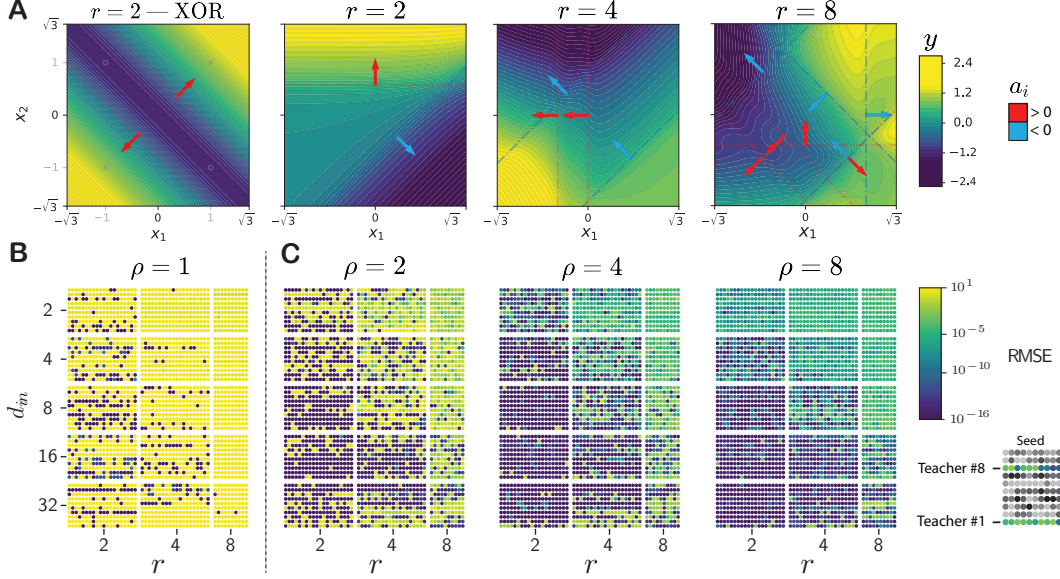


Figure 4: **Artificial data define tasks of variable difficulty.** **A)** For fixed d_{in} , **teacher complexity increases with number r of hidden neurons:** contourplot of the teacher network output $y = b^2 + \sum_i^r a_i g(w_i^T x + b_i^1)$ for $d_{in} = 2$ input dimensions and different r , b^2 denotes the bias of the output unit. Each hidden neuron generates a hyperplane, $w_i^T x + b_i^1 = 0$ (dashed lines); the direction of the weight vector w_i is indicated by an arrow and the sign of the output weight a_i by its color. Top left: generalization of the XOR or parity-bit problem to a regression setting. From left to right: As the number of hidden neurons increases the level lines become more intricate. **B)** **Non-convexity prevents training to zero loss:** for each combination of $d_{in} = 2, 4, 8, 16, 32$ and $r = 2, 4, 8$ we generated 10 teachers; for each teacher, we trained 20 or 10 students (for $r = 8$) with different seeds. Each teacher corresponds to one row of dots while each dot corresponds to one seed (see inset bottom right). Dark blue dots indicate loss below 10^{-14} . Student networks of the same size as the teacher ($\rho = 1$) get often stuck in local minima. The effect is stronger for larger ratios r/d_{in} . **C)** **Effects of overparameterization on convergence:** student networks with overparameterization $\rho \geq 2$ are more likely to converge to near-zero loss than those without. We report the following general trends: (i) overparameterization avoids high loss local minima, (ii) the dataset complexity, i.e. number of hidden neurons per input dimension r/d_{in} , determines the amount of overparameterization needed for reliable convergence to near-zero loss. For difficult teachers, i.e. overcomplete ($r/d_{in} \geq 1$), training is very slow and convergence is not guaranteed in a reasonable amount of time (see Fig. S4).

hidden neurons to reconstruct the layer. We noticed that higher layers align with the teacher weights only at prohibitively low losses [78]. Therefore, if the student networks have more than one hidden layer left to reconstruct, we go back to Step 2 and train again N overparameterized students of $L \leftarrow L - 1$ layers, using as input \mathbf{X} the output of the last reconstructed layer. Repeat this procedure until the last hidden layer is reconstructed (Fig. 3 Algorithm 1, more details in appendix A.5.2).

Step 4: Fine-tuning phase. Adjust the final parameters using the training data.

3.3 Artificial data experiments

We trained overparameterized students on the family of teachers of Section 2.2 with a single hidden layer of r neurons (Figs. 4 and S7). For an overparameterization factor ρ , the student hidden layer has ρr neurons. To stay close to the theoretical setting of near-zero loss and to obtain perfect parameter recovery, we trained all the networks with the package MLPGradientFlow.jl [79]. This allowed us to find global and local minima with machine precision accuracy for networks without overparameterization (Fig. 4B, $\rho = 1$). However, even with second-order ODE solvers and slightly larger networks, it becomes challenging to converge fully to global minima within a reasonable amount of time (Fig. 4C, $\rho \in \{2, 4, 8\}$). Hence, methods to deal with imperfectly trained students are needed. Since training is full-batch (30k data points), the only source of randomness is in the initialization; see

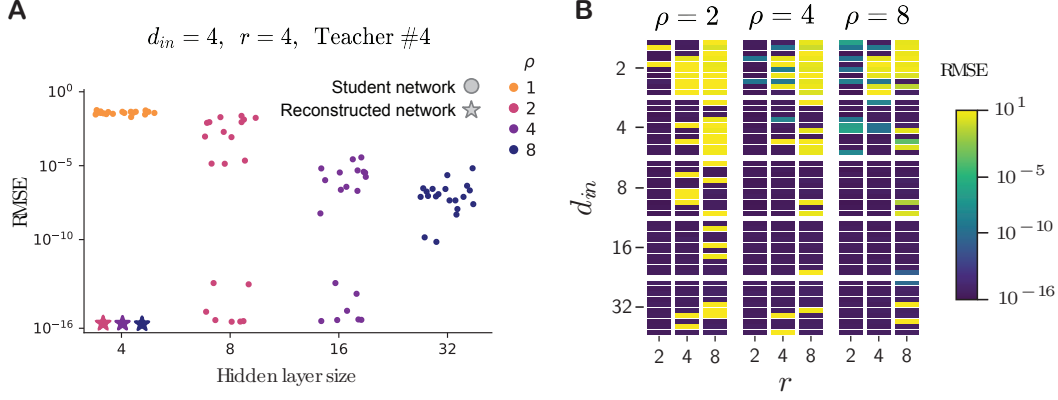


Figure 5: **A) Expand-and-Cluster applied to mildly overparameterized students reaches zero loss:** a total of 80 student networks with 4, 8, 16 or 32 hidden neurons have been trained using data generated by a teacher with $r = 4$ hidden neurons and $d_{in} = 4$ input dimensions. None of the 20 students with 4 hidden neurons reached zero loss (orange dots, $\rho = 1$), while all overparameterized student networks have zero loss with 4 hidden neurons after reconstruction (large colored stars). **B) Loss after Expand-and-Cluster for all teacher networks and student sizes from Figure 4:** the color of each small horizontal bar represents the final loss. Only a small fraction of teacher networks (i.e., those in yellow) were not identified correctly.

appendix A.5 for more details. Figure 4C shows a beneficial trend as overparameterization increases, but also highlights a strong dependence on the dataset (or teacher) complexity r/d_{in} : as the number of hyperplanes per input dimension increases, it becomes harder to train overparameterized students to global minima.

We find that direct training of 20 student networks without overparameterization (data generated from a teacher network with $r = 4$ hidden neurons and input dimensionality $d_{in} = 4$) does not yield a single case of convergence to zero loss (Fig. 5A). For the same teacher, the application of the Expand-and-Cluster algorithm yields student networks that achieve zero loss and hidden-layer size equal to that of the teacher if an overparameterization of $\rho = 2, 4$ or 8 is used in Step 2. This suggests that successful retrieval of all parameters of the teacher network is possible (Fig. 5A).

We tested the quality of parameter identification with Expand-and-Cluster for each teacher network of Figure 4 and illustrate the final loss of the reconstructed networks in Figure 5. For example, of the 30 teacher networks with input dimensionality $d_{in} = 8$, all except 2 networks were correctly identified as indicated by a zero-loss solution (for $\rho = 4, 8$ and $\text{RMSE} \leq 10^{-14}$, dark blue in Fig. 5B). Of 150 different teacher networks, 118 ($\sim 80\%$) were correctly identified with $\rho = 4$. For all correctly identified networks, the maximum angle between the weight vectors of the teacher network and the corresponding vector of the reconstructed student network was less than $3 \cdot 10^{-8}$ radians. In all but 7 out of 118 successful recoveries, the number of neurons found matches that of the teacher; the other cases have at most up to 4 neurons in excess (these can be easily categorized into zero-type and constant-type neurons, see e.g. Fig. S6).

3.4 MNIST shallow and deep experiments

Now we turn to applications using bigger networks where zero-loss solutions are not attainable because of computational time and memory budget, and noise in the optimizer (SGD). Expand-and-Cluster can discern duplicates from zero or constant type neurons that would not be otherwise distinguishable with a simple hard threshold on the weight values and therefore outperforms ‘magnitude pruning’ [23]. We explore the sensitivity of Expand-and-Cluster to the number of students N on the MNIST regression task described in Section 2.3 (Figure 6B). We found that with two students Expand-and-Cluster works reasonably well but does not reliably identify the minimal network. However, with $N \geq 4$ student networks, the Expand-and-Cluster algorithm enabled us to identify the teacher network with at most 5 percent of additional neurons.

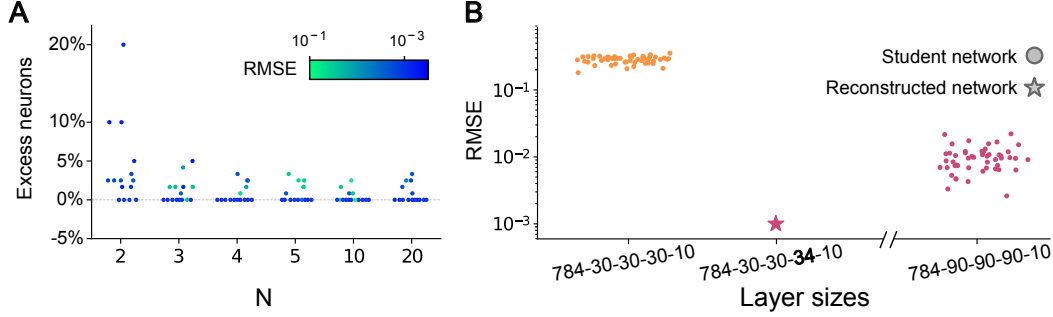


Figure 6: **Parameter recovery for larger networks.** **A) MNIST shallow teachers:** fraction of excess neurons (with respect to the teacher size) clustered as a function of the N students used for Expand-and-Cluster($N, \gamma = 0.5, \beta = \pi/6$). Combined statistics across three shallow teachers of sizes $r \in \{10, 30, 60\}$ pre-trained on MNIST data. **B) MNIST deep teacher:** A fully connected teacher of layer sizes 784-30-30-30-10 trained on MNIST is reconstructed with Expand-and-Cluster($N = 50, \gamma = 0.5, \beta = \pi/5$) applied to students of factor $\rho = 3$ overparameterization (magenta dots) with 4 excess neurons in the last hidden layer (magenta star). Direct training with the teacher network architecture never reached losses below 0.1 (orange dots).

Unlike other methods [12–14], Expand-and-Cluster identifies deep fully connected networks trained on artificial data (see appendix A.3) and larger networks trained on MNIST, Figure 6B. We show a successful reconstruction of three hidden layers of 30 neurons each by applying Expand-and-Cluster to students overparameterized by a factor 3. The reconstruction identifies layer sizes up to 4 neurons in excess for the last hidden layer and achieves a loss of 3 orders of magnitude lower than similar-sized networks trained from random initialization (Fig. 6B). The reconstructed network has a fidelity (fraction of labels matching with the teacher) of 100% and 96.75% on train and test set, respectively.

4 Conclusions

Even if the data is generated by a teacher of known size and architecture, recovering the parameters of the teacher network by training a student network of the same size is difficult to achieve with gradient-descent methods [13]. Indeed, if a student network of the same size as the teacher is trained, it is rare to find the global minimum because of the extreme non-convexity of the loss function: across 1024 training runs of students that contain the same number of hidden neurons as the teacher the global minimum was found only in 2 cases (Fig. S3A). However, using the same computation budget to train 128 students containing $\rho = 8$ times more neurons than the teacher, we reached near zero-loss solutions in 72 cases (56%). For a successful application of the Expand-and-Cluster algorithm, it is desirable to have at least $N = 3$ students near a global minimum. Thus, with the above probability of convergence with an overparameterization of $\rho = 8$, ten students are sufficient to find at least three low-loss solutions with $\sim 95\%$ probability - yet, using the same computation time for 80 runs of the student with the minimal number of hidden units is unlikely to yield even one zero-loss solution. In summary, the detour of expansion-convergence-clustering is a computationally efficient way to find the unique (up to permutations) global minima of a non-convex loss function where standard solution methods rarely work.

Four generalizations of our approach should be straightforward. First, Expand-and-Cluster should work on convolutional layers just as well as it does on dense layers. Second, we obtained our results in a regression setting with a mean square error loss, but the method should also work with the cross-entropy loss as is commonly used in classification settings. Third, our simulation results are obtained with a symmetry-free activation function but, as discussed in Section 3.1, our results can be generalized to common activation functions, if we correctly account for symmetries. Fourth, the choice of dataset should not bring any difference in difficulty as we are dealing with a regression task of data generated by a smaller teacher network. At this stage, our results are limited to simple setups, primarily due to the high computational budget required to reach low losses in more complicated setups. For shallow relu networks, appendix A.4, our method does not reach the same exact extraction accuracy as other methods [12, 13], probably due to the slow finetuning required. In contrast, our method works for arbitrary smooth activation functions and is extendable to deeper networks.

Acknowledgments and Disclosure of Funding

This work was supported by Sinergia Project CRSII5_198612 and SNF Project 200020_207426.

References

- [1] David E Rumelhart, Geoffrey E Hinton, and Ronald J Williams. Learning internal representations by error propagation. In David E Rumelhart, James L McClelland, and PDP Research Group, editors, *Parallel Distributed Processing*, volume 1, chapter 8, pages 318–362. MIT press Cambridge, MA, 1986.
- [2] Song Mei, Yu Bai, and Andrea Montanari. The landscape of empirical risk for nonconvex losses. *The Annals of Statistics*, 46(6A):2747–2774, 2018.
- [3] Spencer Frei, Yuan Cao, and Quanquan Gu. Agnostic learning of a single neuron with gradient descent. *Advances in Neural Information Processing Systems*, 33:5417–5428, 2020.
- [4] Gilad Yehudai and Shamir Ohad. Learning a single neuron with gradient methods. In *Conference on Learning Theory*, pages 3756–3786. PMLR, 2020.
- [5] Arthur Jacot, Franck Gabriel, and Clément Hongler. Neural tangent kernel: Convergence and generalization in neural networks. *Advances in neural information processing systems*, 31, 2018.
- [6] Lenaïc Chizat and Francis Bach. On the global convergence of gradient descent for over-parameterized models using optimal transport. *Advances in neural information processing systems*, 31, 2018.
- [7] Simon S. Du, Xiyu Zhai, Barnabas Póczos, and Aarti Singh. Gradient descent provably optimizes over-parameterized neural networks. In *International Conference on Learning Representations*, 2019.
- [8] Song Mei, Andrea Montanari, and Phan-Minh Nguyen. A mean field view of the landscape of two-layer neural networks. *Proceedings of the National Academy of Sciences*, 115(33):E7665–E7671, 2018.
- [9] Grant Rotskoff and Eric Vanden-Eijnden. Trainability and accuracy of artificial neural networks: An interacting particle system approach. *Communications on Pure and Applied Mathematics*, 75(9):1889–1935, 2022.
- [10] Berfin Şimşek, François Ged, Arthur Jacot, Francesco Spadaro, Clément Hongler, Wulfram Gerstner, and Johanni Brea. Geometry of the loss landscape in overparameterized neural networks: Symmetries and invariances. In *International Conference on Machine Learning*, pages 9722–9732. PMLR, 2021.
- [11] Yaim Cooper. The loss landscape of overparameterized neural networks. *arXiv preprint arXiv:1804.10200*, 2018.
- [12] David Rolnick and Konrad Kording. Reverse-engineering deep relu networks. In *International Conference on Machine Learning*, pages 8178–8187. PMLR, 2020.
- [13] Matthew Jagielski, Nicholas Carlini, David Berthelot, Alex Kurakin, and Nicolas Papernot. High accuracy and high fidelity extraction of neural networks. In *29th USENIX security symposium (USENIX Security 20)*, pages 1345–1362, 2020.
- [14] Massimo Fornasier, Timo Klock, Marco Mondelli, and Michael Rauchensteiner. Finite sample identification of wide shallow neural networks with biases. *arXiv preprint arXiv:2211.04589*, 2022.
- [15] Behnam Neyshabur, Zhiyuan Li, Srinadh Bhojanapalli, Yann LeCun, and Nathan Srebro. Towards understanding the role of over-parametrization in generalization of neural networks. In *International Conference on Learning Representations (ICLR)*, 2019.

- [16] Chiyuan Zhang, Samy Bengio, Moritz Hardt, Benjamin Recht, and Oriol Vinyals. Understanding deep learning (still) requires rethinking generalization. *Communications of the ACM*, 64(3): 107–115, 2021.
- [17] David Saad and Sara A Solla. On-line learning in soft committee machines. *Physical Review E*, 52(4):4225, 1995.
- [18] Sebastian Goldt, Madhu Advani, Andrew M Saxe, Florent Krzakala, and Lenka Zdeborová. Dynamics of stochastic gradient descent for two-layer neural networks in the teacher-student setup. *Advances in neural information processing systems*, 32, 2019.
- [19] Dhruva Venkita Raman, Adriana Perez Rotondo, and Timothy O’Leary. Fundamental bounds on learning performance in neural circuits. *Proceedings of the National Academy of Sciences*, 116(21):10537–10546, 2019.
- [20] Cameron Jakub and Mihai Nica. Depth degeneracy in neural networks: Vanishing angles in fully connected relu networks on initialization. *arXiv preprint arXiv:2302.09712*, 2023.
- [21] Yann LeCun. The mnist database of handwritten digits. <http://yann.lecun.com/exdb/mnist/>, 1998.
- [22] Yann LeCun, John Denker, and Sara Solla. Optimal brain damage. *Advances in neural information processing systems*, 2, 1989.
- [23] Song Han, Jeff Pool, John Tran, and William Dally. Learning both weights and connections for efficient neural network. *Advances in neural information processing systems*, 28, 2015.
- [24] Jonathan Frankle and Michael Carbin. The lottery ticket hypothesis: Finding sparse, trainable neural networks. In *International Conference on Learning Representations*, 2019.
- [25] Torsten Hoefer, Dan Alistarh, Tal Ben-Nun, Nikoli Dryden, and Alexandra Peste. Sparsity in deep learning: Pruning and growth for efficient inference and training in neural networks. *J. Mach. Learn. Res.*, 22(241):1–124, 2021.
- [26] Hengyuan Hu, Rui Peng, Yu-Wing Tai, and Chi-Keung Tang. Network trimming: A data-driven neuron pruning approach towards efficient deep architectures. *arXiv preprint arXiv:1607.03250*, 2016.
- [27] Ben Mussay, Dan Feldman, Samson Zhou, Vladimir Braverman, and Margarita Osadchy. Data-independent structured pruning of neural networks via coresets. *IEEE Transactions on Neural Networks and Learning Systems*, 2021.
- [28] Tianyi Chen, Bo Ji, Tianyu Ding, Biyi Fang, Guanyi Wang, Zhihui Zhu, Luming Liang, Yixin Shi, Sheng Yi, and Xiao Tu. Only train once: A one-shot neural network training and pruning framework. *Advances in Neural Information Processing Systems*, 34:19637–19651, 2021.
- [29] Suraj Srinivas and R. Venkatesh Babu. Data-free parameter pruning for deep neural networks. In *Proceedings of the British Machine Vision Conference (BMVC)*, pages 31.1–31.12, September 2015.
- [30] Zachary Ankner, Alex Renda, Gintare Karolina Dziugaite, Jonathan Frankle, and Tian Jin. The effect of data dimensionality on neural network prunability. *arXiv preprint arXiv:2212.00291*, 2022.
- [31] Stefano Spigler, Mario Geiger, Stéphane d’Ascoli, Levent Sagun, Giulio Biroli, and Matthieu Wyart. A jamming transition from under-to over-parametrization affects generalization in deep learning. *Journal of Physics A: Mathematical and Theoretical*, 52(47):474001, 2019.
- [32] Mario Geiger, Stefano Spigler, Stéphane d’Ascoli, Levent Sagun, Marco Baity-Jesi, Giulio Biroli, and Matthieu Wyart. Jamming transition as a paradigm to understand the loss landscape of deep neural networks. *Physical Review E*, 100(1):012115, 2019.
- [33] Mikhail Belkin, Daniel Hsu, Siyuan Ma, and Soumik Mandal. Reconciling modern machine-learning practice and the classical bias–variance trade-off. *Proceedings of the National Academy of Sciences*, 116(32):15849–15854, 2019.

- [34] Zeyuan Allen-Zhu and Yuanzhi Li. Towards understanding ensemble, knowledge distillation and self-distillation in deep learning. *arXiv preprint arXiv:2012.09816*, 2020.
- [35] Sidak Pal Singh and Martin Jaggi. Model fusion via optimal transport. *Advances in Neural Information Processing Systems*, 33:22045–22055, 2020.
- [36] Hongyi Wang, Mikhail Yurochkin, Yuekai Sun, Dimitris Papailiopoulos, and Yasaman Khazaeni. Federated learning with matched averaging. In *International Conference on Learning Representations*, 2020.
- [37] Norman Tatro, Pin-Yu Chen, Payel Das, Igor Melnyk, Prasanna Sattigeri, and Rongjie Lai. Optimizing mode connectivity via neuron alignment. *Advances in Neural Information Processing Systems*, 33:15300–15311, 2020.
- [38] Rahim Entezari, Hanie Sedghi, Olga Saukh, and Behnam Neyshabur. The role of permutation invariance in linear mode connectivity of neural networks. In *10th International Conference on Learning Representations: ICLR 2022*, 2022.
- [39] Samuel K Ainsworth, Jonathan Hayase, and Siddhartha Srinivasa. Git re-basin: Merging models modulo permutation symmetries. *arXiv preprint arXiv:2209.04836*, 2022.
- [40] Keller Jordan, Hanie Sedghi, Olga Saukh, Rahim Entezari, and Behnam Neyshabur. Repair: Renormalizing permuted activations for interpolation repair. *arXiv preprint arXiv:2211.08403*, 2022.
- [41] Itay Safran and Ohad Shamir. Spurious local minima are common in two-layer relu neural networks. In *International conference on machine learning*, pages 4433–4441. PMLR, 2018.
- [42] Hao Li, Zheng Xu, Gavin Taylor, Christoph Studer, and Tom Goldstein. Visualizing the loss landscape of neural nets. *Advances in neural information processing systems*, 31, 2018.
- [43] Yuqian Zhang, Qing Qu, and John Wright. From symmetry to geometry: Tractable nonconvex problems. *arXiv preprint arXiv:2007.06753*, 2020.
- [44] Jean B Lasserre. Global optimization with polynomials and the problem of moments. *SIAM Journal on optimization*, 11(3):796–817, 2001.
- [45] Hiroshi Ishikawa. Exact optimization for markov random fields with convex priors. *IEEE transactions on pattern analysis and machine intelligence*, 25(10):1333–1336, 2003.
- [46] Sebastien Roy and Ingemar J Cox. A maximum-flow formulation of the n-camera stereo correspondence problem. In *Sixth International Conference on Computer Vision (IEEE Cat. No. 98CH36271)*, pages 492–499. IEEE, 1998.
- [47] Hanif D Sherali and Warren P Adams. A hierarchy of relaxations between the continuous and convex hull representations for zero-one programming problems. *SIAM Journal on Discrete Mathematics*, 3(3):411–430, 1990.
- [48] Egon Balas. Disjunctive programming: Properties of the convex hull of feasible points. *Discrete Applied Mathematics*, 89(1-3):3–44, 1998.
- [49] Tacchi Matteo. Lift and project methods and their application to optimal and optimization-based control. https://cao2022.sciencesconf.org/data/pages/Invited_Session_Proposal_IFAC_CA0_2022_Lift_and_project_methods_and_their_application_to_optimal_and_optimization_based_control.pdf, 2022.
- [50] Milan Korda and Igor Mezić. Linear predictors for nonlinear dynamical systems: Koopman operator meets model predictive control. *Automatica*, 93:149–160, 2018.
- [51] Majid Janzamin, Hanie Sedghi, and Anima Anandkumar. Beating the perils of non-convexity: Guaranteed training of neural networks using tensor methods. *arXiv preprint arXiv:1506.08473*, 2015.

- [52] Yossi Arjevani and Michael Field. Analytic study of families of spurious minima in two-layer relu neural networks: a tale of symmetry ii. *Advances in Neural Information Processing Systems*, 34:15162–15174, 2021.
- [53] Emmanuel Abbe, Elisabetta Cornacchia, Jan Hazla, and Christopher Marquis. An initial alignment between neural network and target is needed for gradient descent to learn. In *International Conference on Machine Learning*, pages 33–52. PMLR, 2022.
- [54] Marco Mondelli and Andrea Montanari. On the connection between learning two-layer neural networks and tensor decomposition. In *The 22nd International Conference on Artificial Intelligence and Statistics*, pages 1051–1060. PMLR, 2019.
- [55] Chris Olah, Arvind Satyanarayan, Ian Johnson, Shan Carter, Ludwig Schubert, Katherine Ye, and Alexander Mordvintsev. The building blocks of interpretability. *Distill*, 3(3):e10, 2018.
- [56] Yu Zhang, Peter Tiño, Aleš Leonardis, and Ke Tang. A survey on neural network interpretability. *IEEE Transactions on Emerging Topics in Computational Intelligence*, 2021.
- [57] Silviu-Marian Udrescu and Max Tegmark. Ai feynman: A physics-inspired method for symbolic regression. *Science Advances*, 6(16):eaay2631, 2020.
- [58] Nelson Elhage, Tristan Hume, Catherine Olsson, Nicholas Schiefer, Tom Henighan, Shauna Kravec, Zac Hatfield-Dodds, Robert Lasenby, Dawn Drain, Carol Chen, Roger Grosse, Sam McCandlish, Jared Kaplan, Dario Amodei, Martin Wattenberg, and Christopher Olah. Toy models of superposition. *Transformer Circuits Thread*, 2022. https://transformer-circuits.pub/2022/toy_model/index.html.
- [59] Adam S Jermyn, Nicholas Schiefer, and Evan Hubinger. Engineering monosemanticity in toy models. *arXiv preprint arXiv:2211.09169*, 2022.
- [60] Stephen Casper, Xavier Boix, Vanessa D’Amario, Ling Guo, Martin Schrimpf, Kasper Vinken, and Gabriel Kreiman. Frivolous units: Wider networks are not really that wide. In *Proceedings of the AAAI Conference on Artificial Intelligence*, volume 35, pages 6921–6929, 2021.
- [61] Daryna Oliynyk, Rudolf Mayer, and Andreas Rauber. I know what you trained last summer: A survey on stealing machine learning models and defences. *arXiv preprint arXiv:2206.08451*, 2022.
- [62] Héctor J Sussmann. Uniqueness of the weights for minimal feedforward nets with a given input-output map. *Neural networks*, 5(4):589–593, 1992.
- [63] Francesca Albertini, Eduardo D Sontag, and Vincent Maillot. Uniqueness of weights for neural networks. *Artificial Neural Networks for Speech and Vision*, pages 115–125, 1993.
- [64] Charles Fefferman. Reconstructing a neural net from its output. *Revista Matemática Iberoamericana*, 10(3):507–555, 1994.
- [65] Pencho P Petrushev. Approximation by ridge functions and neural networks. *SIAM Journal on Mathematical Analysis*, 30(1):155–189, 1998.
- [66] Martin D Buhmann and Allan Pinkus. Identifying linear combinations of ridge functions. *Advances in Applied Mathematics*, 22(1):103–118, 1999.
- [67] Kai Zhong, Zhao Song, Prateek Jain, Peter L Bartlett, and Inderjit S Dhillon. Recovery guarantees for one-hidden-layer neural networks. In *International conference on machine learning*, pages 4140–4149. PMLR, 2017.
- [68] Verner Vlačić and Helmut Bölcskei. Affine symmetries and neural network identifiability. *Advances in Mathematics*, 376:107485, 2021.
- [69] Verner Vlačić and Helmut Bölcskei. Neural network identifiability for a family of sigmoidal nonlinearities. *Constructive Approximation*, 55(1):173–224, 2022.
- [70] Phuong Bui Thi Mai and Christoph Lampert. Functional vs. parametric equivalence of relu networks. In *8th International Conference on Learning Representations*, 2020.

- [71] Pierre Stock and Rémi Gribonval. An embedding of relu networks and an analysis of their identifiability. *Constructive Approximation*, pages 1–47, 2022.
- [72] Joachim Bona-Pellissier, François Bachoc, and François Malgouyres. Parameter identifiability of a deep feedforward relu neural network. *arXiv preprint arXiv:2112.12982*, 2021.
- [73] Nicholas Carlini, Matthew Jagielski, and Ilya Mironov. Cryptanalytic extraction of neural network models. In *Annual International Cryptology Conference*, pages 189–218. Springer, 2020.
- [74] Christian Fiedler, Massimo Fornasier, Timo Klock, and Michael Rauchensteiner. Stable recovery of entangled weights: Towards robust identification of deep neural networks from minimal samples. *Applied and Computational Harmonic Analysis*, 62:123–172, 2023.
- [75] Massimo Fornasier, Jan Vybíral, and Ingrid Daubechies. Robust and resource efficient identification of shallow neural networks by fewest samples. *Information and Inference: A Journal of the IMA*, 10(2):625–695, 2021.
- [76] Haoyu Fu, Yuejie Chi, and Yingbin Liang. Guaranteed recovery of one-hidden-layer neural networks via cross entropy. *IEEE transactions on signal processing*, 68:3225–3235, 2020.
- [77] Massimo Fornasier, Timo Klock, and Michael Rauchensteiner. Robust and resource-efficient identification of two hidden layer neural networks. *Constructive Approximation*, pages 1–62, 2019.
- [78] Yuandong Tian. Student specialization in deep rectified networks with finite width and input dimension. In *International Conference on Machine Learning*, pages 9470–9480. PMLR, 2020.
- [79] Johanni Brea, Flavio Martinelli, Berfin Şimşek, and Wulfram Gerstner. Mlpgradientflow: going with the flow of multilayer perceptrons (and finding minima fast and accurately). *arXiv preprint arXiv:2301.10638*, 2023.
- [80] Dan Hendrycks and Kevin Gimpel. Gaussian error linear units (gelus). *arXiv preprint arXiv:1606.08415*, 2016.
- [81] Prajit Ramachandran, Barret Zoph, and Quoc V Le. Searching for activation functions. *arXiv preprint arXiv:1710.05941*, 2017.
- [82] Diganta Misra. Mish: A self regularized non-monotonic activation function. *arXiv preprint arXiv:1908.08681*, 2019.
- [83] Günter Klambauer, Thomas Unterthiner, Andreas Mayr, and Sepp Hochreiter. Self-normalizing neural networks. *Advances in neural information processing systems*, 30, 2017.
- [84] Fionn Murtagh and Pedro Contreras. Algorithms for hierarchical clustering: an overview. *Wiley Interdisciplinary Reviews: Data Mining and Knowledge Discovery*, 2(1):86–97, 2012.
- [85] Xavier Glorot and Yoshua Bengio. Understanding the difficulty of training deep feedforward neural networks. In *Proceedings of the thirteenth international conference on artificial intelligence and statistics*, pages 249–256. JMLR Workshop and Conference Proceedings, 2010.
- [86] Diederik P Kingma and Jimmy Ba. Adam: A method for stochastic optimization. In *ICLR*, 2015.
- [87] Miron B Kursu and Witold R Rudnicki. Feature selection with the boruta package. *Journal of statistical software*, 36:1–13, 2010.

A Appendix

A.1 Activation functions

A.1.1 Even plus linear activation functions

Considering a neuron with an activation function that can be decomposed into linear plus even terms:

$$a\sigma(wx + b) = ac_1 \cdot (wx + b) + a\sigma_{\text{even}}(wx + b)$$

where c_1 is the slope of the linear approximation around 0. The total contribution of aligned, $+(wx + b)$, and opposite, $-(wx + b)$, student neurons is:

$$\sum_{i \in N^+} a_i \sigma(wx + b) + \sum_{j \in N^-} a_j \sigma(-(wx + b)) = c_1 \underbrace{\left(\sum_{i \in N^+} a_i - \sum_{j \in N^-} a_j \right)}_{\text{Linear}} (wx + b) + \underbrace{\sum_{k \in N^\pm} a_k \sigma_{\text{even}}(wx + b)}_{\text{Even}}$$

where N^+ , N^- , N^\pm contain aligned, opposite or all neuron indices, respectively.

If $\sum_{k \in N^\pm} a_k = 0$, we obtain a *linear-type* group that contributes a linear function to the next layer; to keep an exact mapping of the teacher, there must be another *linear-type* group in the same layer contributing the exact opposite linear term. If $\sum_{k \in N^\pm} a_k = a^*$, then the neuron group is a *linear duplicate-type*, replicating a teacher neuron up to a misaligned linear contribution; that can be accounted for by another linear group in the same layer. An example of different neurons reached by a softplus student is shown in supplementary Figure S6.

A.1.2 Constant plus odd activation functions

Considering a neuron with an activation function that can be decomposed into a constant plus odd term:

$$a\sigma(wx + b) = ac_0 + a\sigma_{\text{odd}}(wx + b)$$

where $c_0 = \sigma(0)$. The total contribution of aligned and opposite student neurons is:

$$\sum_{i \in N^+} a_i \sigma(wx + b) + \sum_{j \in N^-} a_j \sigma(-(wx + b)) = c_0 \underbrace{\sum_{k \in N^\pm} a_k}_{\text{Constant}} + \underbrace{\left(\sum_{i \in N^+} a_i - \sum_{j \in N^-} a_j \right) \sigma_{\text{odd}}(wx + b)}_{\text{Odd}}$$

where N^+ , N^- , N^\pm contain aligned, opposite or all neuron indices, respectively.

If $\sum_{i \in N^+} a_i - \sum_{j \in N^-} a_j = 0$, we obtain a *constant-type* group; to keep an exact mapping of the teacher, the sum of all *constant-type* groups in the same layer and the next layer bias must add up to contribute the original bias of the next layer neuron. If $\sum_{i \in N^+} a_i - \sum_{j \in N^-} a_j = a^*$, then the neuron group is a *duplicate-type*, replicating a teacher neuron up to a misaligned constant contribution; that can be accounted for by other constant groups in the same layer or biases in the next. For tanh, there is no constant contribution term ($c_0 = 0$) while it is the case for sigmoid.

A.1.3 Classification of symmetries in commonly used activation functions

The symmetry-free activation function used in all our experiments is $\text{sigmoid}(4x) + \text{softplus}(x)$, but the method translates easily to other smooth activation functions. Here is a categorization of the most commonly used in the field:

- **Odd:** tanh
- **Odd + constant:** sigmoid
- **Even + linear:** softplus, GELU [80], Swish [81]
- **No symmetries** sigmoid + softplus, $\text{sigmoid}(x) + \text{sigmoid}(x + b)$, Mish [82]
- **Not C^∞ :** ReLU, LeakyReLU, SELU [83]

A.1.4 GELU is even + linear

We indicate the n^{th} derivative of a function as $f^{(n)}$. By computing all the derivatives of GELU one can show that it is indeed composed of a linear and even term:

$$\begin{aligned} \text{GELU}(x) &= x \cdot \frac{1}{2} \left[1 + \text{erf} \left(\frac{x}{\sqrt{2}} \right) \right] \\ \text{GELU}^{(1)}(x) &= \frac{1}{2} \left[1 + \text{erf} \left(\frac{x}{\sqrt{2}} \right) + x \cdot \text{erf}^{(1)} \left(\frac{x}{\sqrt{2}} \right) \right] \\ \text{GELU}^{(2)}(x) &= \frac{1}{2} \left[2 \cdot \text{erf}^{(1)} \left(\frac{x}{\sqrt{2}} \right) + x \cdot \text{erf}^{(2)} \left(\frac{x}{\sqrt{2}} \right) \right] \\ &\vdots \\ \text{GELU}^{(n)}(x) &= \frac{1}{2} \left[n \cdot \text{erf}^{(n-1)} \left(\frac{x}{\sqrt{2}} \right) + x \cdot \text{erf}^{(n)} \left(\frac{x}{\sqrt{2}} \right) \right] \end{aligned}$$

Since $\text{erf}(0) = 0$ and $\text{erf}^{(2n)}(0) = 0 \forall n \in \mathbb{N}$, we have that $\text{GELU}^{(2n+1)}(0) = 0 \forall 2n+1 > 1, n \in \mathbb{N}$ and $\text{GELU}^{(1)}(0) = 1/2$.

A.2 Expand-and-Cluster detailed procedure

The input weight vectors of all neurons in a given layer of N mildly overparameterized students are clustered with hierarchical clustering [84] using the average linkage function $\ell(\mathcal{A}, \mathcal{B}) = \frac{1}{|\mathcal{A}| \cdot |\mathcal{B}|} \sum_{i \in \mathcal{A}} \sum_{j \in \mathcal{B}} S_{ij}$, where $S_{ij} = \|w_i - w_j\|_2$ and w_i and w_j are input weight vectors of neurons in the same layer but potentially from different students (Fig. 3B). To identify the clusters of teacher neurons we look for the appropriate height h to cut the dendrogram resulting from hierarchical clustering (Fig. 3C). With $K(h) = \{\kappa_1, \kappa_2, \dots\}$ the set of clusters at threshold h , and $|\kappa_i|$ the size of cluster i , we define the set $C(h, \gamma N) = \{\kappa_i \in K(h) \mid |\kappa_i| \geq \gamma N\}$ of clusters larger than a fraction $\gamma \in (0, 1]$ of the number of students N . For $\gamma > 1/N$, the set $C(h, \gamma N)$ usually does not contain small clusters of zero or offbound type neurons, because they are not aligned between different students. We cut the dendrogram at the height that maximizes the number of big clusters: $\tilde{h} = \arg \max_h |C(h, \gamma N)|$. The set $C(\tilde{h}, \gamma N)$ may still contain clusters of non-aligned neurons whose input weights are close in Euclidean distance (e.g. approximate constant-type neurons with $\|w_i\|$ near zero) but not aligned in angle. Therefore we remove clusters whose within-cluster median angle is higher than β . Each remaining cluster is then collapsed into a single hidden neuron with a winner-take-all policy: we choose the weight vector(s) that belong to the best-performing student in the cluster. Note that if multiple output weights a_1, \dots, a_q of the same network belong to the same cluster, they can be combined into a single output weight $a = \sum_i a_i$, following the definition of duplicate neurons (Fig. 2). If the best student duplicates a given teacher neuron more than once, we take their average. Alternatively, we have also tried to average over all neurons in each cluster and obtained a similar final performance. The hyperparameters of Expand-and-Cluster (N, γ, β) used for each experiment are summarized in appendix A.5.4.

The biases could approximately be reconstructed by identifying all the constant-type neurons, but we found this procedure somewhat brittle. Instead, we fine-tune all bias parameters (keeping constant the weight vectors) with a few steps of gradient descent on the reconstructed network. After each layer reconstruction we retrain N students with fixed non-trainable reconstructed layers but learnable biases, and the remaining layers are overparameterized and learnable. In this retraining phase, we monitor the learned bias values b_k^n of the last reconstructed layer, if the same neuron k learns different bias values across different students n ($\text{std}_n(b_k^n) > 0.1$) we consider that neuron badly clustered and therefore remove it from the layer. We repeat this procedure until the last hidden layer, the final output layer can be reconstructed by simply retrieving the output weights of the last hidden layer neurons. Optionally, to reach machine precision alignment with the teacher, further fine-tuning can be performed.

A.3 Recovery of deep artificial teacher networks

We built two and three hidden layers networks by stacking the procedure to generate artificial teachers presented in the main text (Section 2.2) and detailed in appendix A.5.2. Expand-and-Cluster *without retraining step at each layer reconstruction* was applied to these networks: the reconstructed networks have one or two superfluous neurons for the two and three layer teachers, respectively; (Fig. S1). We emphasize that the final loss of the pruned student networks is at least 8 orders of magnitudes lower than the loss of the best out of 10 students trained with the *correct* number of neurons in each of the hidden layers. Thus, running 10 training runs with student networks overparameterized by a factor of $\rho = 8$ enables us to correctly identify or nearly identify the teacher network, while direct training was not successful with the same number of runs (Fig. S1). Detailed explanations on training and reconstruction are explained in the following sections (appendix A.5.2 and appendix A.5.4).

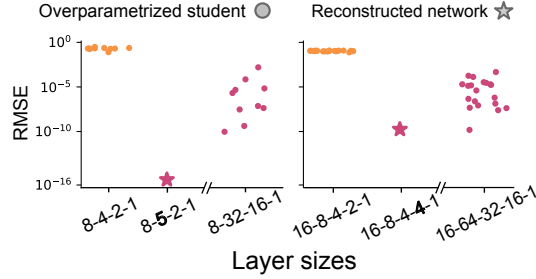


Figure S1: **Deep artificial teachers:** a teacher with input dimension 8, a first hidden layer with 4 neurons, and a second hidden layer with 2 neurons, and a single output (denoted as 8-4-2-1, left) was constructed by stacking the procedure of Figure 4 and generated data to train students of overparameterization $\rho = 8$ (denoted as 8-32-16-1). Similarly, a teacher with architecture 16-8-4-2 (right) generated data to train students with architecture 16-64-32-16. Expand-and-Cluster applied to students trained with an overparameterization of $\rho = 8$ identified the teacher network with one additional neuron in the first hidden layer (left) or with two additional neurons in the third hidden layer (right). In both cases, the loss is below 10^{-10} whereas direct training with the ‘correct’ network architecture never reached a loss below 10^{-2} .

A.4 Recovery of shallow ReLU teacher networks on MNIST

In this section, we show an example of recovery of shallow ReLU network trained on MNIST. Expand-and-Cluster needs to be adapted in order to account for the positive scaling symmetry of the relu function, i.e a $\text{ReLU}(\mathbf{w} \cdot \mathbf{x} + b) = \frac{1}{c} \text{ReLU}(c(\mathbf{w} \cdot \mathbf{x} + b))$. Therefore in this experiment, the clustering is done purely on the angles between weight vectors by using the cosine distance as a similarity metric. The network was reconstructed from students overparametrized by $\rho = 4$ and using Expand-and-Cluster($N = 50, \gamma = 0.75, \beta = \pi/5$). The reconstructed network has a fidelity (fraction of labels matching with the teacher) of 100% and 95.35% on train and test set, respectively. We note that the fidelity results are not on par with Jagielski et al. [13] despite the very low loss achieved, we think these metrics could be improved by further finetuning.

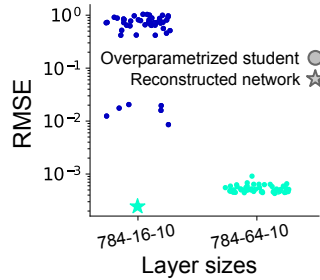


Figure S2: **Shallow ReLU MNIST teachers:** Expand-and-Cluster can be adapted to reconstruct shallow ReLU networks by clustering on the angle between student weight vectors.

A.5 Training and reconstruction details

A.5.1 Toy regression tasks

To explore overparameterized networks trained to exact zero-loss or up to machine precision (for Float64 machine precision is at 10^{16}), we integrated the gradient flow differential equation $\dot{\theta}(t) = -\nabla \mathcal{L}(\theta(t), \mathcal{D})$ with ODE solvers, where \mathcal{L} is the mean square error loss. Specifically, we used the package `MLPGradientFlow.jl` [79] to follow the gradient with high accuracy and exact or approximate second-order methods to fine-tune convergence to a local or global minimum. All of the toy model networks are trained with Float64 precision on CPU machines (Intel Xeon Gold 6132 on Linux machines).

The networks of Figure 4 were trained on an input dataset \mathbf{X} of 30k data points drawn from a uniform distribution between $-\sqrt{3}$ and $+\sqrt{3}$ and targets y computed by the teacher network on the same input \mathbf{X} . Students were initialized following the Glorot normal distribution, mean 0 and $\text{std} = \sqrt{\frac{2}{f_{\text{an_in}} + f_{\text{an_out}}}}$ [85]. We allocated a fixed amount of iteration steps per student: 5000 steps of the ODE solver `KenCarp58` for all networks, plus an additional 5000 steps of exact second order method `NewtonTrustRegion` for non-overparameterized networks ($\rho = 1$) or 250 steps of BFGS for overparameterized networks ($\rho \geq 2$). The stopping criteria for the second training phase were: mean square error loss $\leq 10^{-31}$ or gradient norm $\|\nabla \mathcal{L}(\theta(t))\| \leq 10^{-16}$. Each iteration step is full-batch, the only source of randomness in a student network is its initialization.

The networks shown in Figure 5, after reconstruction, were fine-tuned for a maximum of 15 minutes with `NewtonTrustRegion` if the number of parameters was below or equal to 32 or `LD_SLSQP` otherwise.

A.5.2 Artificial deep networks

The construction of deep teacher networks follows the same mechanism as described in Section 2.2, with the additional extra step of scaling the weights such that each unit of the successive layer receives standardized inputs, analogous to what batch-norm would do for a full batch. This procedure ensures that the input support to each layer does not drift to values that are off-bounds with respect to where each hidden neuron hyperplane is placed. Classically trained networks also follow this scheme to have useful activations, but it is crucial to avoid potential support drift in arbitrarily constructed deep networks.

Toy deep students were trained on a dataset generated in the same way as their shallow counterparts. We allocated 3 hours to solve the gradient flow ODE with `Runge-Kutta4` followed by 6 to 12 hours of approximate second-order optimization with BFGS. After reconstruction, we gave 60 minutes of time budget to fine-tune with `LD_SLSQP` (Fig. 6A).

A.5.3 MNIST teachers and students

Several teachers with a single hidden layer of 10, 30 or 60 neurons were trained with the activation function defined in appendix A.1 to best classify the MNIST dataset by minimizing the cross-entropy loss with the Adam optimizer [86] and early stopping criterion. For each hidden-layer size, the best-performing teacher was used to train the students, see Figure S4A. The student networks were trained to replicate the teacher logits (activation values before being passed to the softmax function) by minimizing a mean square error loss. Students were initialized with the Glorot uniform distribution, ranging from $-a$ to a , where $a = \sqrt{\frac{6}{f_{\text{an_in}} + f_{\text{an_out}}}}$. The training was performed with the Adam optimizer on mini-batches of size 640 with an adaptive learning rate scheduler that reduces the learning rate after more than 100 epochs of non-decreasing training loss. A maximum of 25k epochs was allocated to train these students on GPU machines (NVIDIA Tesla V100 32G). For the layerwise reconstruction of deep teacher networks, every retraining was given a maximum of 10k epochs.

The reconstructed networks shown in Figure 6B are fine-tuned with the same optimizing recipe for a maximum of 2000 epochs. For deep reconstructed networks, a final finetuning of 15k epochs was performed on all the parameters.

A.5.4 Expand-and-Cluster hyperparameters

The Expand-and-Cluster procedure has only 3 hyperparameters to tune: the number of student networks N , the cutoff threshold to eliminate small clusters γ and the maximally admitted alignment angle β .

- **Shallow artificial teachers:** all the procedure was performed with $N = 10$ (for $r = 8$) or $N = 20$ (for $r = 2, 4$), $\gamma = 0.8$ and $\beta = \pi/24$.
- **Deep artificial teachers:** we reconstructed the artificial deep networks *without the retraining step at each layer reconstruction*. This required looser conditions, especially for the higher layers: for the artificial deep networks of 2 hidden layers: $N = 10$, $\gamma = 0.4$ and $\beta = 1 - \arccos(0.01) \simeq 8^\circ$; for the 3 hidden layer case: $N = 20$, $\gamma = 1/3$, $\beta \simeq 0.26^\circ$ for the first layer and $\beta \simeq 30^\circ$ for the other layers. The alignment gets quickly lost as depth increases, motivating the looser β angles. We found this procedure too brittle and decided to modify the algorithm into the version in the main paper (Fig. 3) by adding the retraining step at each layer reconstruction. The reconstruction results for deep MNIST teachers follow this updated algorithm.
- **Shallow MNIST teachers:** for MNIST student networks we notice that no alignment of weight vectors can be expected for the corner pixels of the images because these pixels have the same value for nearly all input images. This prevents weights connected to corner pixels to move from the random initialization. Therefore we removed the uninformative pixels using the tree-based feature importance method Boruta [87] to identify with statistical significance the informative features; the resulting map is shown in Figure S4B. The parameters used for Expand-and-Cluster on MNIST shallow networks of Figure 6B are $\gamma = 0.5$ and $\beta = \pi/6$ while N sweeps from 2 to 20.
- **Deep MNIST teacher:** all the procedure was performed with $N = 50$, $\gamma = 0.5$ and $\beta = \pi/5$ for every layer. Layerwise reconstruction alternated to training of new students is a much more stable procedure than the one described for deep artificial teachers as there is no need to tune the Expand-and-Cluster parameters for every layer.

A.6 Supplementary figures

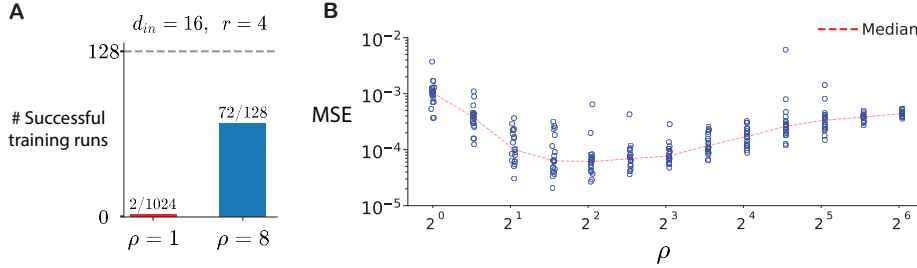


Figure S3: **A) Overparameterization performance scales beyond simple linear parameter scaling:** we successfully retrieve an identical input-output mapping of the original network with a student of the same size ($\rho = 1$) only 2 times out of 1024 runs. If we instead train 8 times fewer networks ($n = 128$) that are 8 times bigger ($\rho = 8$) we achieve a significant improvement in success rate, 72 out of 128 runs. Note that the computational budget of the two experiments is equal. Example shown with teacher configuration $d_{in} = 16$, $r = 4$, teacher #7. **B) Probing expansion factors:** It is impossible to know the overparameterization factor of a student if the teacher is unknown. Nevertheless, one can probe different student sizes with quick training runs of stochastic gradient descent to identify a suitable student size that gives minimal losses. With a fixed time budget per training run, we notice an increase in MSE for large overparameterization.

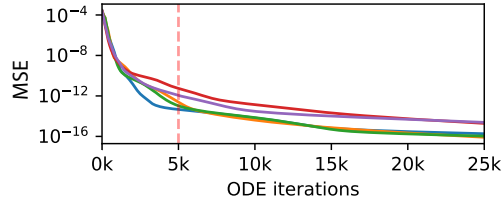


Figure S4: **Training longer slowly decreases student loss for difficult teachers:** the results shown in Figure 4 for difficult teachers are not at convergence despite the large amount of ODE solver steps dedicated (5K for every simulation). If training is continued we can see a slow decrease in loss, hinting that a very complex landscape is generated by difficult teachers. This simulation took more than a day to compute. Each color corresponds to a different student loss curve, the teacher used was of $d_{in} = 2, r = 8$.

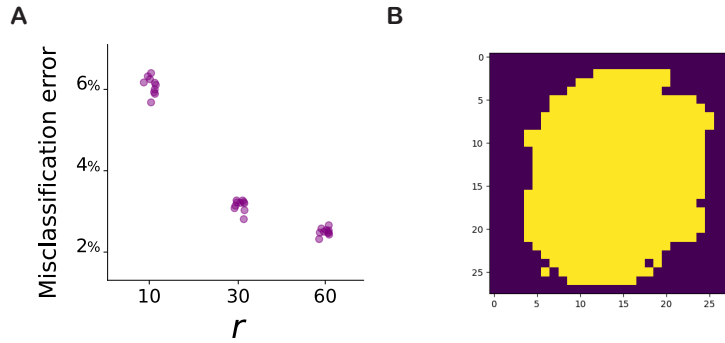


Figure S5: **A) MNIST teachers misclassification error on test set. B) MNIST important pixels mask obtained with BORUTA [87]:** only connections projecting from yellow pixels are considered for the Expand-and-Cluster procedure.

TEACHER

Neuron#	w ₁	w ₂	w ₃	w ₄	b	a
1	0.0798	-0.1591	-1.1932	0.1544	-0.4069	-0.6425
2	0.0885	0.0562	1.4687	-0.0843	1.8938	-3.2114
3	0.5641	-1.2116	-0.9090	0.5318	0.0863	1.3291
4	-1.0788	-1.1397	-0.0288	0.7331	0.7795	1.3658

Final layer bias: 1.4088

STUDENT

Neuron#	w ₁	w ₂	w ₃	w ₄	b	a	
1	0.0000	-0.0000	-0.0002	0.0000	0.0745	0.5669	■
2	-1.0788	-1.1397	-0.0288	0.7331	0.7795	1.3658	■
3	0.3933	-0.4649	-0.1984	0.1733	0.0283	-0.0000	■
4	-0.0381	0.0759	0.5690	-0.0736	0.1359	0.5343	■
5	-0.0798	0.1591	1.1932	-0.1544	0.4052	-0.2547	■
6	0.0675	-0.0581	-0.1721	0.1226	-0.0294	-0.0000	■
7	0.0000	0.0000	0.0000	0.0000	0.0518	0.2907	■
8	0.0049	0.0391	0.6151	-0.0676	-0.0452	-0.0000	■
9	0.0798	-0.1591	-1.1932	0.1544	-0.4079	-0.3878	■
10	0.5641	-1.2116	-0.9090	0.5318	0.0863	1.3291	■
11	-0.0001	0.0001	0.0002	-0.0001	0.1579	0.2025	■
12	0.0381	-0.0759	-0.5690	0.0736	-0.1359	-0.5343	■
13	0.0885	0.0562	1.4687	-0.0843	-2.0982	-3.2114	■
14	0.0000	-0.0000	-0.0003	0.0001	0.0881	0.5097	■
15	-0.2952	0.0844	0.3304	0.0897	0.0357	-0.0000	■
16	0.6287	0.6561	0.1238	-0.3991	-0.4162	-0.0000	■

Final layer bias: 0.2826.

■	Duplicate-type
■	Linear duplicate-type
■	Linear-type
■	Constant-type
■	Zero-type

Figure S6: **Example parameters of a softplus teacher and student:** the table above shows the parameters of a $d_{in} = 4, r = 4$ softplus teacher. The table below shows the parameters of a student of $\rho = 4$ trained on the defined teacher to $\text{RMSE} \sim 10^{-11}$. At a near-zero loss, we can classify all the different neurons (color coded) composing the student, following the classification scheme of Figure 2. Note that the presence of a linear duplicate type implies the presence of a linear type, this group of 4 neurons (blue and purple coded) collaborates to replicate teacher neuron #1.

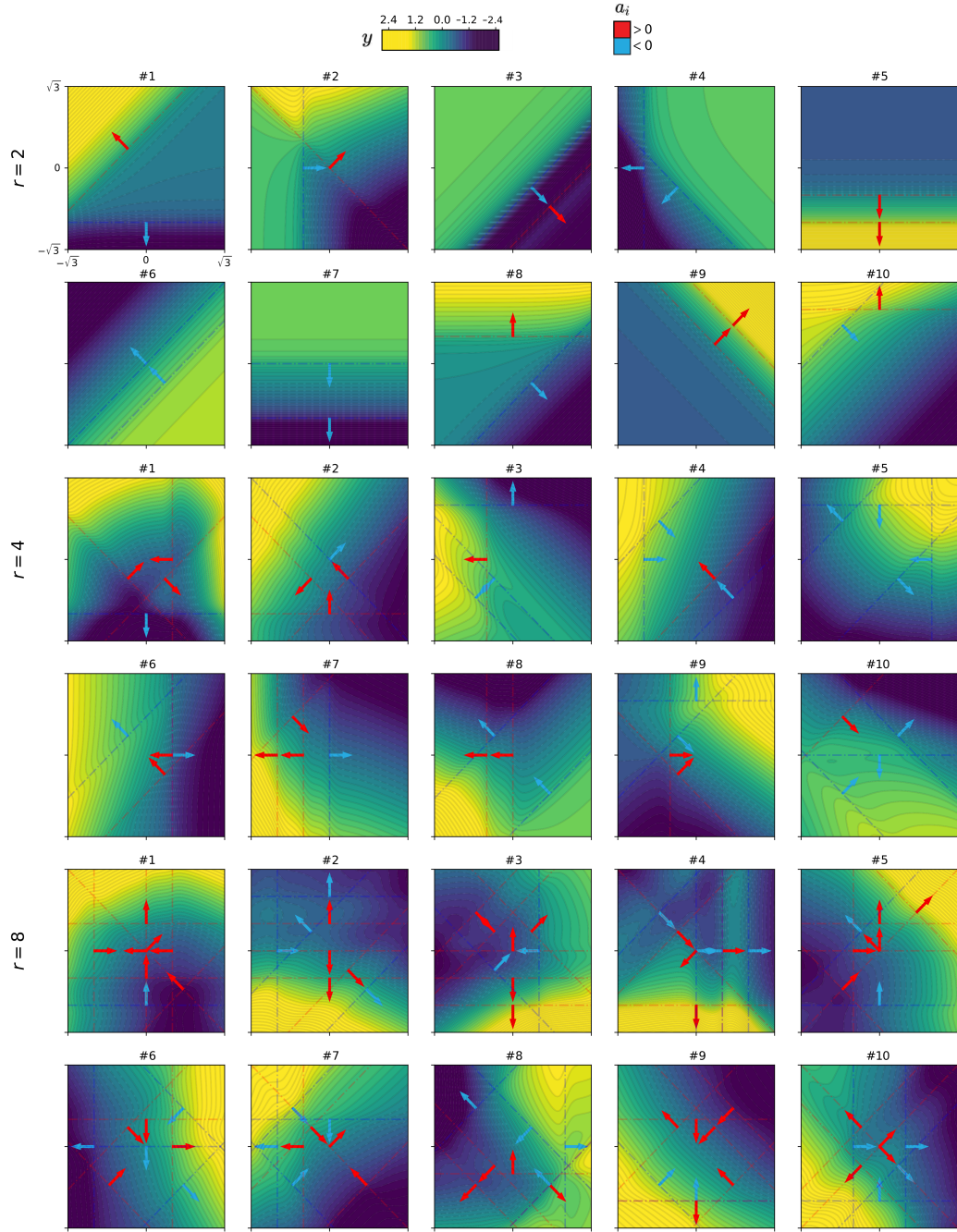


Figure S7: Visualization of all $d_{\text{in}} = 2$ teachers used for results in Figure 4 and 5